ISSN 1063-7834, Physics of the Solid State, 2020, Vol. 62, No. 2, pp. 384–387. © Pleiades Publishing, Ltd., 2020.
Russian Text © The Author(s), 2020, published in Fizika Tverdogo Tela, 2020, Vol. 62, No. 2, pp. 332–335.

GRAPHENES

Structure and Thermodynamic Properties of the $SmGaGe_2O_7$ Oxide

L. T. Denisova[a, *], M. S. Molokeev[a, b], L. A. Irtyugo[a], V. V. Beletskii[a], N. V. Belousova[a], and V. M. Denisov[a]

[a] *Siberian Federal University, Krasnoyarsk, 660041 Russia*

[b] *Kirensky Institute of Physics, Krasnoyarsk Scientific Center, Siberian Branch, Russian Academy of Sciences, Krasnoyarsk, 660036 Russia*

**e-mail: antluba@mail.ru*

Received September 16, 2019; revised September 16, 2019; accepted September 16, 2019

Abstract—The $SmGaGe_2O_7$ oxide material has been obtained from initial Sm_2O_3, Ga_2O_3, and GeO_2 oxides by solid-phase synthesis with annealing in air in the temperature range of 1273–1473 K. The structure of the investigated germanate (sp. gr. $P2_1/c$, a = 7.18610(9) Å, b = 6.57935(8) Å, and c = 12.7932(2) Å) has been established by X-ray diffraction and the high-temperature heat capacity has been determined by differential scanning calorimetry. Using the experimental data on $C_p = f(T)$, the thermodynamic properties of the compound have been calculated.

Keywords: samarium gallium germanate, structure, heat capacity

DOI: 10.1134/S1063783420020109

1. INTRODUCTION

Recently, there has been a steady interest of researchers in germanium-based oxide materials with the general formula $RMGe_2O_7$ (R = rare-earth element (REE), Y; M = Al, Ga, In, Fe) [1–4] due to their application potential. The $RGaGe_2O_7$ are the most underexplored germanates of this class and only fragmentary data on their structure and absorption-luminescent properties are available [5, 6]. Among these materials is the $SmGaGe_2O_7$ oxide. In the literature, data on its heat capacity and thermodynamic properties are lacking. In addition, the phase relations in the Sm_2O_3–Ga_2O_3–GeO_2 system have been understudied. The thermodynamic modeling of phase equilibria and establishing optimal synthesis conditions require data that are currently unavailable.

Therefore, it seemed necessary to study the structure and high-temperature heat capacity and determine the thermodynamic properties of $SmGaGe_2O_7$ using the obtained data.

2. EXPERIMENTAL

The $SmGaGe_2O_7$ compound was obtained from initial Sm_2O_3, Ga_2O_3 (high-purity), and GeO_2 (99.996%) oxides by the solid-phase synthesis. After grinding of the precalcined oxides taken in a stoichiometric ratio, they were tableted without a binder and then fired in air sequentially at 1273 (40 h), 1373 (100 h), and 1473 K (70 h). To ensure the completeness of the solid-state reaction, the sintered tablets were ground every 20 h and pressed again. Since the relatively high temperatures of the solid-state synthesis lead to the evaporation of $GeCO_2$ [7], firing was performed in lidded crucibles. The synthesis time and GeO_2 amount introduced over the stoichiometry were selected experimentally. The phase composition of the obtained samples was controlled by X-ray structural analysis.

An X-ray powder diffraction pattern of $SmGaGe_2O_7$ was obtained on a Bruker D8 ADVANCE diffractometer using a VANTEC linear detector (CuK_α radiation)

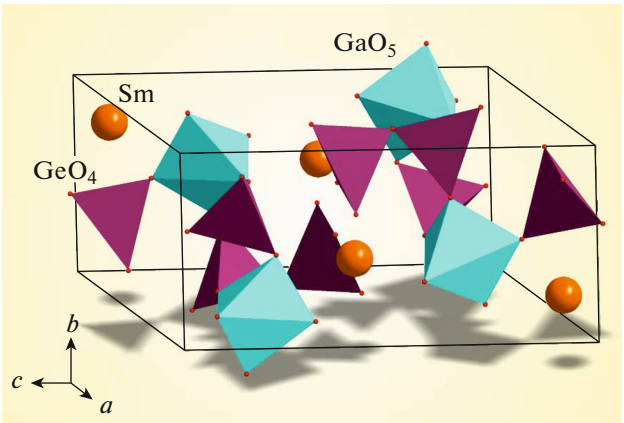

Fig. 1. Crystal structure of $SmGaGe_2O_7$.

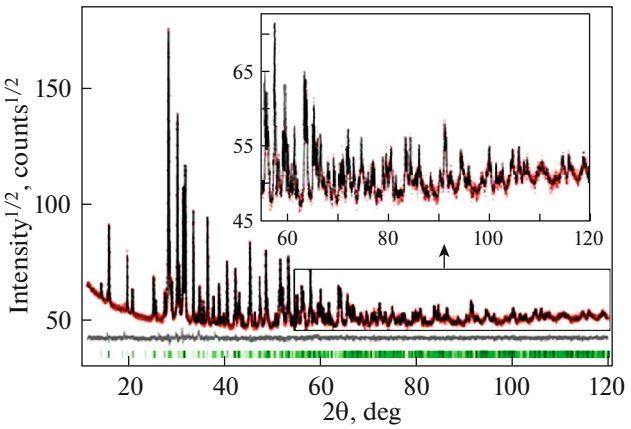

Fig. 2. Rietveld refinement difference X-ray diffraction pattern for $SmGaGe_2O_7$.

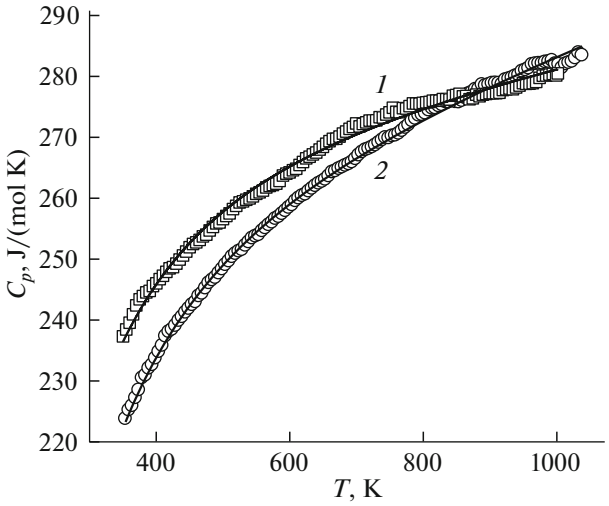

Fig. 3. Temperature dependences of the molar heat capacity for (*1*) $Sm_2Ge_2O_7$ and (*2*) $SmGaGe_2O_7$.

at room temperature. The 2θ angle scanning step was 0.016° and the exposure time was 2 s per step.

The heat capacity of $SmGaGe_2O_7$ was measured on a NETZSCH STA 449 C Jupiter device (Germany). The experimental technique is similar to that described in [8]. The experimental error was no more than 2%.

3. EXPERIMENTAL RESULTS

It was found that the $SmGaGe_2O_7$ oxide is isostructural to the $GdGaGe_2O_7$ compound, the structure of which was established in [5]. Therefore, the atomic coordinates of the latter were taken as a starting model for the Rietveld refinement using the TOPAS 4.2 program [9]. For the conversion, the Gd site was replaced by a Sm ion (Fig. 1). The refinement yielded low uncertainty factors (see Table 1 and Fig. 2).

The atomic coordinates and main bond lengths for $SmGaGe_2O_7$ are given in Tables 2 and 3, respectively. The comparison of the $SmGaGe_2O_7$ unit cell parameters obtained by us (Table 1) with the data from [5] (a = 7.18(1) Å, b = 6.56(1) Å, c = 12.79(1) Å, β = 117.4(2)°, and d = 5.93 g/cm^3) shows their good agreement.

Figure 3 presents the temperature dependence of the heat capacity of $SmGaGe_2O_7$. It can be seen that, with an increase in temperature from 350 to 1000 K, the C_p values expectedly grow and the dependence $C_p = f(T)$ contains no extrema. The latter is apparently indicative of the absence of polymorphic transformations in $SmGaGe_2O_7$ in the investigated temperature range. The data obtained can be described by the classical Maier–Kelley equation

$$C_p = a + bT - cT^{-2}, \quad (1)$$

which has the following form for $SmGaGe_2O_7$:

$$C_p = (250.39 \pm 0.69) + (37.78 \pm 0.70) \times 10^{-3} T - (50.73 \pm 0.77) \times 10^5 T^{-2}. \quad (2)$$

The correlation coefficient in Eq. (2) is 0.9992 and the maximum deviation of the experimental points form the smoothing curve is 0.66%.

Table 1. Main parameters of shooting and refinement of the $SmGaGe_2O_7$ crystal structure (sp. gr. $P2_1/c$)

Parameter	Value
a, Å	7.18610(9)
b, Å	6.57935(8)
c, Å	12.7932(2)
β, deg	117.4216(6)
V, Å^3	536.90(1)
Z	4
d, g/cm^3	5/90
2θ angle range, deg	10–120
R_{wp}, %	2.34
R_p, %	1.81
R_{exp}, %	1.87
χ^2	1.25
R_B, %	0.46

a, b, c, and β are the unit cell parameters; V is the cell volume; d is the calculated density; R_{wp}, R_p, R_{exp}, and R_B are the weight profile, profile, expected, and integral uncertainty factors, respectively; χ^2 is the fitting quality, and Z is the number of structural units.

Table 2. Atomic coordinates and isotropic heat parameters B_{iso} of the $SmGaGe_2O_7$ structure

Atom	x	y	z	B_{iso}
Sm	0.7607(2)	0.14692(19)	0.02485(12)	0.39(13)
Ga1	0.7893(4)	0.3998(5)	0.2689(2)	0.41(13)
Ge1	0.7837(4)	0.6566(4)	0.0435(2)	0.20(14)
Ge2	0.2993(4)	0.4100(4)	0.2215(2)	0.35(14)
O1	0.5896(18)	0.8308(19)	0.0191(9)	0.29(17)
O2	0.7782(15)	0.115(2)	0.2181(10)	0.29(17)
O3	0.5674(16)	0.383(2)	0.3064(10)	0.29(17)
O4	0.0047(18)	0.3285(19)	0.4208(10)	0.29(17)
O5	0.746(2)	0.0005(16)	0.4226(11)	0.29(17)
O6	0.7947(18)	0.4488(15)	0.1307(11)	0.29(17)
O7	0.154(2)	0.1867(17)	0.1870(12)	0.29(17)

Table 3. Main bond lengths (Å) in the $SmGaGe_2O_7$ structure

Bond length	Value	Bond length	Value
$Sm-O1^{(I)}$	2.400(12)	$Ga1-O4^{(VI)}$	1.903(11)
$Sm-O1^{(II)}$	2.318(8)	Ga1–O6	1.815(12)
Sm–O2	2.426(10)	$Ga1-O7^{(VII)}$	1.959(12)
$Sm-O3^{(III)}$	2.490(11)	Ge1–O1	1.719(10)
$Sm-O4^{(IV)}$	2.576(11)	$Ge1-O4^{(VII)}$	1.777(10)
$Sm-O4^{(V)}$	2.650(8)	$Ge1-O5^{(III)}$	1.773(12)
$Sm-O5^{(III)}$	2.641(11)	Ge1–O6	1.743(11)
Sm–O6	2.352(11)	$Ge2-O2^{(VII)}$	1.767(11)
$Sm-O7^{(VI)}$	2.640(11)	Ge2–O3	1.731(8)
Ga1–O2	1.973(13)	$Ge2-O5^{(VII)}$	1.819(12)
Ga1–O3	1.869(7)	Ge2–O7	1.737(11)

The symmetry elements are (I) $x, y-1, z$; (II) $-x+1, -y+1, -z$; (III) $x, -y+1/2, z-1/2$, (IV) $-x+1/2, y-1/2, -z+1/2$; (V) $x+1, -y+1/2, z-1/2$; (VI) $x+1, y, z$; and (VII) $-x+1, y+1/2, -z+1/2$.

Table 4. Thermodynamic properties of $SmGaGe_2O_7$

T, K	C_p, J/(mol K)	$H^0(T) - H^0(350\ K)$, kJ/mol	$S^0(T) - S^0(350\ K)$, J/(mol K)	$\Phi^0(T)$, J/(mol K)
350	222.2	–	–	–
400	233.8	11.42	30.47	1.93
450	242.3	23.33	58.52	6.68
500	249.0	35.20	84.41	13.18
550	254.4	48.21	108.4	20.76
600	259.0	61.04	130.7	29.00
650	262.9	74.09	151.6	37.64
700	266.5	87.33	171.3	46.49
750	269.7	100.7	189.7	55.43
800	272.7	114.3	207.3	64.38
850	275.5	128.0	223.9	73.27
900	278.1	141.8	239.7	82.08
1000	283.1	169.9	269.3	99.34

We could not compare our data on the heat capacity of $SmGaGe_2O_7$ with results obtained by other authors because of a lack of such data. Therefore, Fig. 3 shows the data for $Sm_2Ge_2O_7$ [10]. It can be seen that the partial substitution of gallium for samarium leads generally to a decrease in heat capacity. Only at $T \geq 900$ K, the C_p values become comparable.

Using Eq. (2), we calculated the thermodynamic functions of $SmGaGe_2O_7$ (the enthalpy change $H^0(T) - H^0(350\ K)$, the entropy change $S^0(T) - S^0(350\ K)$, and the reduced Gibbs energy $\Phi^0(T)$) from the known thermodynamic relations. The results are given in Table 4.

It follows from Table 4 that the C_p values at $T > 800$ K exceed the Dulong–Petit limit $3Rs$, where R is the universal gas constant and s is the number of atoms per formula unit of the oxide compound ($s = 11$).

4. CONCLUSIONS

Using the solid phase reaction, the $SmGaGe_2O_7$ compound has been synthesized, its crystal structure was refined, and its high-temperature heat capacity

was studied. It was established that the experimental values of $C_p = f(T)$ are well-described by the Maier–Kelley equation. The thermodynamic functions of the oxide compound were calculated.

FUNDING

This study was carried out within the state assignment of the Ministry of Science and Higher Education of the Russian Federation to the Siberian Federal University in 2017–2019, project no. 4.8083.2017/8.9 "Formation of a Data Bank of Thermodynamic Characteristics of the Complex-Oxide Multifunctional Materials Containing Rare and Scattered Elements."

CONFLICT OF INTEREST

The authors declare that they have no conflicts of interest.

REFERENCES

1. E. A. Juárez-Arellano, L. Bucio, J. L. Ruvalcaba, R. Moreno-Tovar, J. E. Garcia-Robledo, and E. Oroxco, Z. Kristallogr. **217**, 201 (2002).
2. A. A. Kaminskii, H. Rhee, O. Lux, A. Kaltenbach, H. J. Eichler, J. Hanuza, S. N. Bagayev, H. Uonea, A. Shirakawa, and K. Ueda, Laser Phys. Lett. **10**, 075803 (2013).
3. T. V. Drokina, G. A. Petrakovskii, D. A. Velikanov, and M. S. Molokeev, Phys. Solid State **56**, 1131 (2014).
4. L. T. Denisova, Yu. F. Kargin, L. A. Irtyugo, N. V. Belousova, V. V. Beletskii, and V. M. Denisov, Inorg. Mater. **54**, 1245 (2018).
5. A. A. Kaminskii, B. V. Mill, A. V. Butashin, E. L. Belokoneva, and K. Rurbanov, Phys. Status Solidi A **103**, 575 (1987).
6. G. Lozano, C. Cascales, and P. Porcher, J. Alloys Compd. **303**, 349 (2000).
7. V. W. Becker and J. Felsche, J. Less-Comm. Met. **128**, 269 (1987).
8. L. T. Denisova, L. A. Irtyugo, Yu. F. Kargin, V. V. Beletskii, and V. M. Denisov, Inorg. Mater. **53**, 93 (2017).
9. *Bruker AXS TOPAS V4: General Profile and Structure Analysis Software for Powder Diffraction Data, User's Manual* (Bruker AXS, Karlsruhe, Germany, 2008).
10. L. T. Denisova, L. A. Irtyugo, Yu. F. Kargin, V. V. Beletskii, N. V. Belousova, and V. M. Denisov, Inorg. Mater. **54**, 167 (2018).

Translated by E. Bondareva